

# Awakening the Sleeping Carboxylase Function of Enzymes: Engineering the Natural CO<sub>2</sub>-Binding Potential of Reductases

Iria Bernhardsgrütter,<sup>†</sup> Kristina Schell,<sup>†</sup> Dominik M. Peter,<sup>†</sup> Farshad Borjian,<sup>‡</sup> David Adrian Saez,<sup>§</sup> Esteban Vöhringer-Martinez,<sup>§</sup> and Tobias J. Erb<sup>\*,†,||</sup>

<sup>†</sup>Department of Biochemistry and Synthetic Metabolism, Max Planck Institute for Terrestrial Microbiology, Karl-von-Frisch-Straße 10, D-35043 Marburg, Germany

<sup>‡</sup>Institute for Molecular Microbiology and Biotechnology, University of Münster, Corrensstr. 3, D-48149 Münster, Germany

<sup>§</sup>Departamento de Físico Química, Facultad de Ciencias Químicas, Universidad de Concepción, 1290 Concepción, Chile

<sup>||</sup>LOEWE Center for Synthetic Microbiology (Synmikro), Karl-von-Frisch-Straße 16, D-35043 Marburg, Germany

## Supporting Information

**ABSTRACT:** Developing new carbon dioxide (CO<sub>2</sub>) fixing enzymes is a prerequisite to create new biocatalysts for diverse applications in chemistry, biotechnology and synthetic biology. Here we used bioinformatics to identify a “sleeping carboxylase function” in the superfamily of medium-chain dehydrogenases/reductases (MDR), i.e. enzymes that possess a low carboxylation side activity next to their original enzyme reaction. We show that propionyl-CoA synthase from *Erythrobacter* sp. NAP1, as well as an acrylyl-CoA reductase from *Nitrosopumilus maritimus* possess carboxylation yields of  $3 \pm 1$  and  $4.5 \pm 0.9\%$ . We use rational design to engineer these enzymes further into carboxylases by increasing interactions of the proteins with CO<sub>2</sub> and suppressing diffusion of water to the active site. The engineered carboxylases show improved CO<sub>2</sub>-binding and kinetic parameters comparable to naturally existing CO<sub>2</sub>-fixing enzymes. Our results provide a strategy to develop novel CO<sub>2</sub>-fixing enzymes and shed light on the emergence of natural carboxylases during evolution.

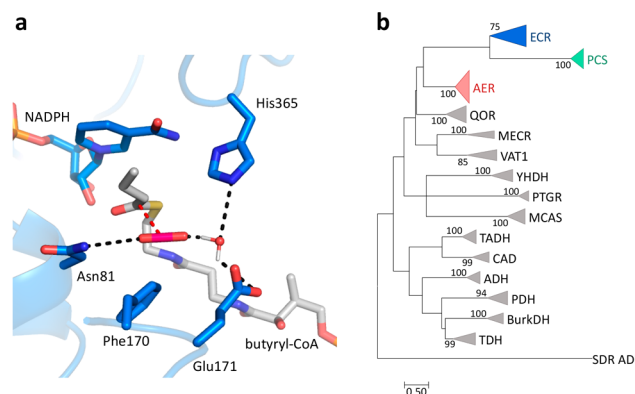


**Figure 1.** CO<sub>2</sub>-binding pocket of ECR and its partial conservation in the MDR superfamily. (a) Active site of ECR<sub>Ks</sub>.<sup>7</sup> The CO<sub>2</sub>-binding pocket is defined by four conserved residues (Asn81, Phe170, Glu171, His365). CO<sub>2</sub> was modeled into the structure. (b) Maximum-likelihood tree of the MDR superfamily<sup>9</sup> with (potential) CO<sub>2</sub>-binding enzyme families highlighted in color.

To harvest atmospheric CO<sub>2</sub> as a sustainable carbon source for (bio)catalytic and (bio)technological applications,<sup>1–5</sup> it is necessary to extend the repertoire of CO<sub>2</sub>-fixing reactions. One possibility is to engineer a carboxylation function into the scaffold of non-CO<sub>2</sub>-fixing enzymes. Generally, the interaction of CO<sub>2</sub> with proteins is poorly understood.<sup>6</sup> However, for enoyl-CoA carboxylase/reductase from *Kitasatospora setae* (ECR<sub>Ks</sub>), four conserved amino acids that form a CO<sub>2</sub>-binding pocket at the active site were described recently<sup>7</sup> (Figure 1a). These four amino acids anchor and position the CO<sub>2</sub> molecule during catalysis, in which a reactive enolate is formed that attacks the CO<sub>2</sub>.<sup>8</sup>

To identify enzyme scaffolds capable of binding CO<sub>2</sub> beyond the ECR enzyme family, we searched homologues of the MDR superfamily for the CO<sub>2</sub>-binding motif. Our search revealed two enzyme families that show the potential to bind CO<sub>2</sub>, the propionyl-CoA synthase (PCS) and an archaeal enoyl-CoA reductase (AER) family (Figure 1b). The PCS family clusters closely to ECRs and shows a fully conserved CO<sub>2</sub>-binding

motif across individual family members (Figure S1). The AER family is more distantly related to the ECR family, and selected homologues only contain one or two of the four conserved residues of the CO<sub>2</sub>-binding pocket (Figure S2). We decided to test selected members of these enzyme families in their CO<sub>2</sub>-fixing capabilities.

PCS is a three-domain fusion enzyme that catalyzes the overall conversion of 3-hydroxypropionate to propionyl-CoA<sup>10</sup> (Figure 2a). The enzyme forms a central reaction chamber, in which three subsequent reactions take place in a synchronized fashion.<sup>11</sup> When we assayed PCS from *Erythrobacter* sp. NAP1, PCS<sub>EN</sub>, at 4.4 mM dissolved CO<sub>2</sub>, we detected minor amounts of methylmalonyl-CoA besides the main product propionyl-CoA. Incorporation of <sup>13</sup>CO<sub>2</sub>-label confirmed the latent carboxylation activity of PCS<sub>EN</sub> (Figure 2b). Notably, the carboxylation function was not limited to the *Erythrobacter* enzyme, but was also detected with PCS from *Chloroflexus aurantiacus* (PCS<sub>Ca</sub>, Table S1).

Received: April 10, 2019

Published: June 12, 2019

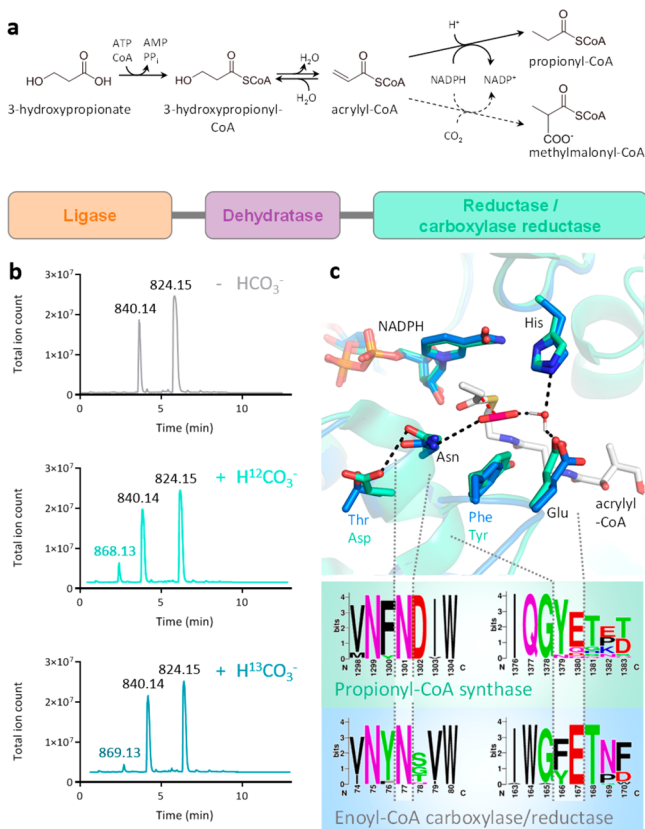


**Figure 2.** PCS<sub>EN</sub> possesses a “sleeping carboxylase function”. (a) Reaction sequence of PCS. PCS natively catalyzes the conversion of 3-hydroxypropionate into propionyl-CoA (solid lines) and possesses a low carboxylation activity yielding methylmalonyl-CoA (dashed line). (b) High-performance liquid chromatography-mass spectrometry traces of the PCS<sub>EN</sub> overall reaction showing 3-hydroxypropionyl-CoA, propionyl-CoA and (3-<sup>12/13</sup>C)-methylmalonyl-CoA at *m/z* 840.14, 824.15 and 868.13/869.13, respectively. Methylmalonyl-CoA is only detected in the presence of <sup>12/13</sup>CO<sub>2</sub> (provided as bicarbonate). Data represent an individual experiment with two replicates. (c) Active site of PCS<sub>EN</sub> reductase domain (cyan, PDB: 4EQO<sup>11</sup>) and ECR<sub>Ks</sub> (blue<sup>7</sup>), both cocrystallized with NADP<sup>+</sup>. Acrylyl-CoA and CO<sub>2</sub> are modeled into the active site. WebLogo-illustration<sup>12,13</sup> of conserved active site residues using 129 PCS and 29 ECR sequences. Numbering according to PCS<sub>EN</sub> or ECR<sub>Ks</sub>, respectively.

The last reaction in the three-reaction sequence of PCS is the reduction of acrylyl-CoA to propionyl-CoA, catalyzed by a reductase domain harboring the CO<sub>2</sub>-binding motif (Figure 2a,c). We directly tested the reductase domain for carboxylation activity with an E1027Q variant of PCS<sub>EN</sub> (PCS<sub>EN</sub><sub>ΔDH</sub>) that is unable to generate acrylyl-CoA. When PCS<sub>EN</sub><sub>ΔDH</sub> was provided with external acrylyl-CoA and 4.4

mM dissolved CO<sub>2</sub>, the enzyme showed a carboxylation yield (defined as percentage yield of carboxylated product compared with total product formed, including reduced side product) of 3 ± 1% (Table 1). This showed that the reductase domain is able to carboxylate acrylyl-CoA directly.

To improve further the carboxylation efficiency of PCS<sub>EN</sub>, we compared the active site of PCS<sub>EN</sub> (PDB: 6EQO) with ECR<sub>Ks</sub>. While the NADPH binding site, as well as the four CO<sub>2</sub>-binding pocket residues are structurally conserved (Figure 2c), we noticed differences in the second shell of the active site. ECR<sub>Ks</sub> features a small hydrophilic residue (Thr82), which interacts with Asn81 that stabilizes CO<sub>2</sub> through its carboxamide NH<sub>2</sub> group. The corresponding residue in PCS<sub>EN</sub> is occupied by an aspartate (Asp1302). Molecular dynamics (MD) simulations demonstrated that Asp1302 in PCS<sub>EN</sub> forms a strong anionic hydrogen bond to the carboxamide NH<sub>2</sub> group of Asn1301 (Figures 3a and S5),

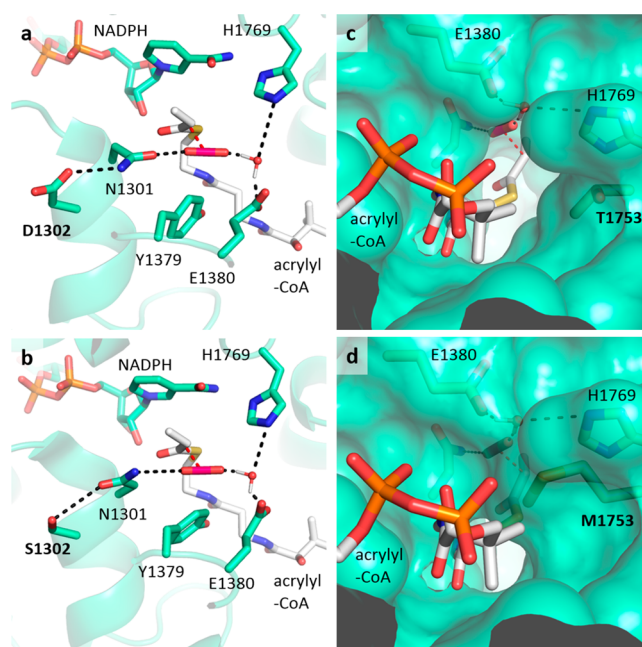


**Figure 3.** Directed mutagenesis to exploit the carboxylation activity of PCS<sub>EN</sub>. (a) Representative snapshot from the MD simulation of the active site in wild type PCS<sub>EN</sub>. (b) Active site model of PCS<sub>EN</sub> D1302S to unlock Asn1301. (c) Active site of wild type PCS<sub>EN</sub>. (d) Active site model of PCS<sub>EN</sub> T1753M to restrict water access to the active site. Acrylyl-CoA and CO<sub>2</sub> were modeled into the active site.

locking Asn1301 in a position which prevents interactions with CO<sub>2</sub>. This finding is in line with the fact that we could not determine an apparent *K<sub>M</sub>* for CO<sub>2</sub> with PCS<sub>EN</sub><sub>ΔDH</sub> and that

**Table 1.** Reaction Parameters and Carboxylation Yield for the Reductase Domain of Different PCS<sub>EN</sub> Variants<sup>a</sup>

PCS variant	app. <i>k</i> <sub>cat</sub> (s <sup>-1</sup> ) at 4.4 mM CO <sub>2</sub>	app. <i>K</i> <sub>M,acrylyl-CoA</sub> (mM)	% carboxylation at 4.4 mM CO <sub>2</sub>	app. <i>K</i> <sub>M,CO2</sub> (mM)
PCS <sub>EN</sub> <sub>ΔDH</sub> WT	7.4 ± 1.0	0.014 ± 0.002	3 ± 1	n.m.
PCS <sub>EN</sub> <sub>ΔDH</sub> D1302S	1.77 ± 0.09	0.027 ± 0.003	20.9 ± 0.7	27 ± 5
PCS <sub>EN</sub> <sub>ΔDH</sub> T1753M	6.5 ± 0.6	0.0197 ± 0.0012	10 ± 2	n.m.
PCS <sub>EN</sub> <sub>ΔDH</sub> D1302S T1753M	0.46 ± 0.03	0.026 ± 0.003	69 ± 3	26 ± 5

<sup>a</sup>*k*<sub>cat</sub> shows combined reduction and carboxylation activity. *K<sub>M</sub>* values were determined from a Michaelis–Menten fit of at least 18 data points, with fixed acrylyl-CoA concentrations for *K<sub>M,CO2</sub>* (Figures S3 and S4, Table S2 for *k*<sub>cat</sub> values). Carboxylation yields are calculated from mean carboxylation yields over five time points in three replicates. Data are mean ± s.d. CO<sub>2</sub> concentrations were calculated. n.m., not measurable.

replacing Asn1301 by an aspartate abolished carboxylation activity.

We aimed at unlocking Asn1301 from its fixed position by replacing Asp1302 with different small hydrophilic residues. PCS<sub>EN-ΔDH</sub> variant D1302S (Figure 3b) showed an increased carboxylation yield of  $20.9 \pm 0.7\%$  at 4.4 mM dissolved CO<sub>2</sub>, and notably also Michaelis–Menten-like behavior with CO<sub>2</sub> at an apparent  $K_{M\_CO_2}$  of  $27 \pm 5$  mM (Table 1). Together with MD simulations that showed a more flexible asparagine residue (Figure S5) this demonstrated that unlocking Asn1301 improves CO<sub>2</sub>-binding and carboxylation efficiency in PCS<sub>EN</sub>.

Another, equally important catalytic principle in carboxylases is the exclusion of water from the active site to minimize protonation reactions which would prematurely quench C–C bond formation.<sup>7,14–16</sup> In ECR<sub>Ks</sub>, a conserved methionine (Met356) restricts access of water to the CO<sub>2</sub>-binding pocket. In PCS<sub>EN</sub>, this residue is a threonine, which presumably allows water to enter the active site and displace the CO<sub>2</sub> molecule (Figure 3c). When we introduced the methionine in PCS<sub>EN</sub> (PCS<sub>EN-ΔDH</sub> T1753M, Figure 3d), carboxylation yield increased to  $10 \pm 2\%$  at 4.4 mM dissolved CO<sub>2</sub>. When combining the D1302S with the T1753M mutation, the carboxylation yield of PCS<sub>EN-ΔDH</sub> further increased up to  $69 \pm 3\%$  at 4.4 mM CO<sub>2</sub> (Table 1). Under saturating CO<sub>2</sub> concentrations (i.e., 44 mM CO<sub>2</sub>), PCS<sub>EN-ΔDH</sub> D1302S T1753M showed a carboxylation yield of  $94.5 \pm 0.7\%$ , demonstrating that we successfully converted the reductase domain into a carboxylase. During engineering, the  $k_{cat}$  of reduction was strongly decreased, while the apparent  $k_{cat}$  for carboxylation was maintained (Table S2) and falls in the range of naturally existing ECRs.<sup>4,17</sup> The engineered carboxylase domain also improved carboxylation yield in the context of the overall reaction of PCS<sub>EN</sub> (Supporting Information I).

We next investigated the carboxylation potential in the AER enzyme family of unknown function. We chose Nmar\_1565 (AER<sub>Nm</sub>), a homologue from *Nitrosopumilus maritimus*, in which two of the four amino acids of the CO<sub>2</sub>-binding motif, namely Phe122 and Glu123, are conserved (Figure 4a,b). Although no function was assigned to AER<sub>Nm</sub> so far, we speculated that the enzyme might catalyze the reduction of acrylyl-CoA in the 3-hydroxypropionate/4-hydroxybutyrate cycle of *N. maritimus*.<sup>18,19</sup> Indeed, the enzyme reduced acrylyl-CoA to propionyl-CoA at an apparent  $k_{cat}$  of  $0.99 \pm 0.11$  s<sup>−1</sup>, confirming its reductase function.

AER<sub>Nm</sub> activity was very sensitive to salt and buffer composition (Supporting Information II). When we incubated the enzyme with NaHCO<sub>3</sub>, at concentrations corresponding to 1.31 mM free CO<sub>2</sub>, activity dropped 10-fold. However, under these conditions AER<sub>Nm</sub> showed a latent carboxylation activity and converted acrylyl-CoA into methylmalonyl-CoA at a carboxylation yield of  $4.5 \pm 0.9\%$  (Table 2), despite the lack of two of the four amino acid residues of the CO<sub>2</sub>-binding motif. To increase the carboxylation efficiency of AER<sub>Nm</sub> we decided to rebuild the CO<sub>2</sub>-binding pocket through introduction of asparagine and histidine. Reintroduction of histidine failed due to inactive protein, which might be a result of interrupted second-shell interactions to Thr307 or steric clashes. However, replacing Asp50 by asparagine increased carboxylation yield dramatically (to  $82 \pm 5\%$ , Figure 4c, Table 2). The increase in catalytic activity in AER<sub>Nm</sub> D50N was accompanied by an improved  $K_{M\_CO_2}$  ( $0.18 \pm 0.03$  mM), indicating increased CO<sub>2</sub>-binding. AER<sub>Nm</sub> D50N performed best in 100 mM phosphate buffer, where it showed  $k_{cat}$  and carboxylation yields

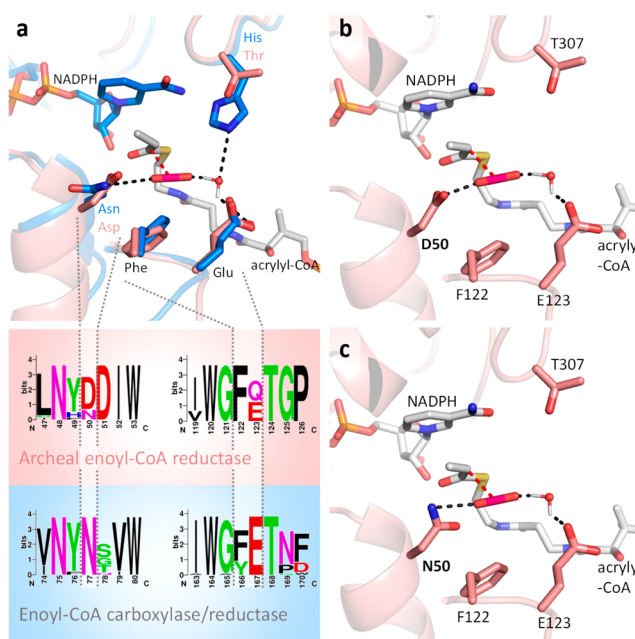


**Figure 4.** Awakening the “sleeping carboxylase function” in AER<sub>Nm</sub>. (a) Active sites of AER<sub>Nm</sub> (salmon) and ECR<sub>Ks</sub> (blue). Illustration of conserved active site residues, generated by WebLogo<sup>12,13</sup> using 21 AER<sub>Nm</sub> and 29 ECR sequences. Residue numbering refers to AER<sub>Nm</sub> or ECR<sub>Ks</sub>, respectively. (b) Model of the AER<sub>Nm</sub> wild type active site carrying an Asp50 instead of a conserved Asn. (c) Model of the AER<sub>Nm</sub> D50N active site. Homology models were created with an ECR from *Streptomyces* sp. NRRL 2288 (PDB: 4y0k<sup>21</sup>) using SWISS-MODEL.<sup>22</sup> Acrylyl-CoA and CO<sub>2</sub> were modeled into the active site.

**Table 2. Reaction Parameters and Carboxylation Yield for AER<sub>Nm</sub> Variants in 100 mM KHPO<sub>4</sub> (pH 7.5)<sup>a</sup>**

AER variant	app. $k_{cat}$ (s <sup>−1</sup> ) at 1.31 mM CO <sub>2</sub>	% carboxylation at 1.31 mM CO <sub>2</sub>	$K_{M\_CO_2}$ (mM)
WT	$0.084 \pm 0.011$	$4.5 \pm 0.9$	n.m.
D50N	$1.6 \pm 0.2$	$82 \pm 5$	$0.18 \pm 0.03$

<sup>a</sup> $k_{cat}$  shows combined carboxylation and reduction activity.  $K_{M\_CO_2}$  values were determined from a Michaelis–Menten fit of at least 18 data points with a fixed concentration of acrylyl-CoA (Figure S6, Table S3 for  $k_{cat}$  values). Carboxylation yields were calculated from the mean carboxylation ratio over five time points in three replicates. Data are mean  $\pm$  s.d. CO<sub>2</sub> concentrations were calculated. n.m., not measurable.

comparable to those of naturally existing carboxylases, such as RubisCO<sup>20</sup> (Table 2).

In conclusion, we successfully reshaped the energy landscape of acrylyl-CoA reductases from the thermodynamically favored product propionyl-CoA ( $\Delta_r G'^0 \approx -63$  kJ/mol) to the disfavored methylmalonyl-CoA ( $\Delta_r G'^0 \approx -43$  kJ/mol).<sup>23</sup> Our engineering efforts show that improving CO<sub>2</sub>-binding (reduced energy barrier for carboxylation) and minimizing side reaction with water (increased energy barrier for reduction) are both required to establish a carboxylation activity in the scaffold of different reductases. This is in line with the idea that in catalysis stabilization of favorable transition states (“positive catalysis”) and destabilization of unwanted transition states (“negative catalysis”) are both important,<sup>24–26</sup> as further supported by the finding that suppression of competing protonation side reactions is essential for efficient CO<sub>2</sub>-fixation



in ECR<sub>Ks</sub> and 2-ketopropyl coenzyme M oxidoreductase/carboxylase.<sup>14–16</sup>

On a broader picture, our findings also raise questions about the emergence of natural carboxylases. How did carboxylation functions naturally evolve in the scaffold of proteins, such as RubisCO or ECR? It has been suggested that these enzymes originated from non-CO<sub>2</sub>-fixing ancestors.<sup>27,28</sup> Our data provides experimental evidence for this evolutionary scenario by demonstrating that the MDR superfamily, to which ECR belongs, naturally possesses the capacity to interact with the CO<sub>2</sub>-molecule. It apparently takes only a few mutations to transform latent carboxylases that convert CO<sub>2</sub> at low efficiency and nonphysiological CO<sub>2</sub> concentrations into decent CO<sub>2</sub>-fixing enzymes.

Another apparent question is why PCS and AER would possess a “sleeping carboxylase function”? One explanation might be that the latent carboxylation activity was selected for. PCS operates in the 3-hydroxypropionate bicycle in *C. aurantiacus* and a modified version thereof in *Erythrobacter* sp. NAP1 (Figure S7a),<sup>29,30</sup> while AER<sub>Nm</sub> presumably works in the 3-hydroxypropionate/4-hydroxybutyrate cycle in *N. maritimus* (Figure S7b).<sup>18</sup> Bioenergetic considerations suggest that even a low carboxylation activity would increase biomass yield of these organisms, which thrive at a constantly low energy supply<sup>18</sup> (Supporting Information III).

In summary, our proof-of-principle study demonstrates that it is possible to exploit the active site of reductases to create novel carboxylases. This opens the possibility for the future engineering of novel CO<sub>2</sub>-fixing enzymes that could find application in biocatalysis and synthetic biology (e.g., in artificial pathways for the conversion of CO<sub>2</sub><sup>31,32</sup>).

## ■ ASSOCIATED CONTENT

### ■ Supporting Information

The Supporting Information is available free of charge on the ACS Publications website at DOI: 10.1021/jacs.9b03431.

Experimental details, biochemical enzyme characterization, compound synthesis, analytical HPLC methods, bioinformatics methods, supporting figures and tables (PDF)

## ■ AUTHOR INFORMATION

### Corresponding Author

\*toerb@mpi-marburg.mpg.de

### ORCID

David Adrian Saez: 0000-0001-5555-8720

Esteban Vöhringer-Martinez: 0000-0003-1785-4558

Tobias J. Erb: 0000-0003-3685-0894

### Notes

The authors declare no competing financial interest.

## ■ ACKNOWLEDGMENTS

We thank Gabriele Stoffel for his input on the mechanism of CO<sub>2</sub>-binding in ECRs and Niña Socorro Cortina for operating the hrLC-MS. The work conducted by the U.S. Department of Energy Joint Genome Institute, a DOE Office of Science User Facility, is supported under Contract No. DE-AC02-05CH11231. This work was funded by the Deutsche Forschungsgemeinschaft through Collaborative Research Centre SFB 987, the European Research Council (ERC 637675 “SYBORG”), the Gebert-Rüf-Stiftung (GRS 062-12),

the Max-Planck-Society Partnergroup Program and the Max-Planck-Society.

## ■ REFERENCES

- (1) Glueck, S. M.; Gümüş, S.; Fabian, W. M.; Faber, K. Biocatalytic carboxylation. *Chem. Soc. Rev.* **2010**, *39*, 313–328.
- (2) Martin, J.; Eisoldt, L.; Skerra, A. Fixation of gaseous CO<sub>2</sub> by reversing a decarboxylase for the biocatalytic synthesis of the essential amino acid L-methionine. *Nat. Catal.* **2018**, *1*, 555.
- (3) Plasch, K.; Hofer, G.; Keller, W.; Hay, S.; Heyes, D. J.; Dennig, A.; Glueck, S. M.; Faber, K. Pressurized CO<sub>2</sub> as a carboxylating agent for the biocatalytic *ortho*-carboxylation of resorcinol. *Green Chem.* **2018**, *20*, 1754–1759.
- (4) Peter, D. M.; Schada von Borzyskowski, L.; Kiefer, P.; Christen, P.; Vorholt, J. A.; Erb, T. J. Screening and Engineering the Synthetic Potential of Carboxylating Reductases from Central Metabolism and Polyketide Biosynthesis. *Angew. Chem., Int. Ed.* **2015**, *54*, 13457–13461.
- (5) Zhang, L.; Mori, T.; Zheng, Q.; Awakawa, T.; Yan, Y.; Liu, W.; Abe, I. Rational Control of Polyketide Extender Units by Structure-Based Engineering of a Crotonyl-CoA Carboxylase/Reductase in Antimycin Biosynthesis. *Angew. Chem., Int. Ed.* **2015**, *54*, 13462–13465.
- (6) Cundari, T. R.; Wilson, A. K.; Drummond, M. L.; Gonzalez, H. E.; Jorgensen, K. R.; Payne, S.; Braundfeld, J.; De Jesus, M.; Johnson, V. M. CO<sub>2</sub>-formatics: how do proteins bind carbon dioxide? *J. Chem. Inf. Model.* **2009**, *49*, 2111–2115.
- (7) Stoffel, G. M. M.; Saez, D. A.; DeMirci, H.; Vögeli, B.; Rao, Y.; Zarzycki, J.; Yoshikuni, Y.; Wakatsuki, S.; Vöhringer-Martinez, E.; Erb, T. J. Four amino acids define the CO<sub>2</sub> binding pocket of enoyl-CoA carboxylases/reductases. *Proc. Natl. Acad. Sci. U.S.A.* **2019**, in press.
- (8) Rosenthal, R. G.; Ebert, M.-O.; Kiefer, P.; Peter, D. M.; Vorholt, J. A.; Erb, T. J. Direct evidence for a covalent ene adduct intermediate in NAD (P) H-dependent enzymes. *Nat. Chem. Biol.* **2014**, *10*, 50.
- (9) Hedlund, J.; Jörnvall, H.; Persson, B. Subdivision of the MDR superfamily of medium-chain dehydrogenases/reductases through iterative hidden Markov model refinement. *BMC Bioinf.* **2010**, *11*, 534.
- (10) Alber, B. E.; Fuchs, G. Propionyl-coenzyme A synthase from *Chloroflexus aurantiacus*, a key enzyme of the 3-hydroxypropionate cycle for autotrophic CO<sub>2</sub> fixation. *J. Biol. Chem.* **2002**, *277*, 12137–12143.
- (11) Bernhardsgrütter, I.; Vögeli, B.; Wagner, T.; Peter, D. M.; Cortina, N. S.; Kahnt, J.; Bange, G.; Engilberge, S.; Girard, E.; Riobé, F.; et al. The multicatalytic compartment of propionyl-CoA synthase sequesters a toxic metabolite. *Nat. Chem. Biol.* **2018**, *14*, 1127.
- (12) Crooks, G. E.; Hon, G.; Chandonia, J.-M.; Brenner, S. E. WebLogo: a sequence logo generator. *Genome Res.* **2004**, *14*, 1188–1190.
- (13) Schneider, T. D.; Stephens, R. M. Sequence logos: a new way to display consensus sequences. *Nucleic Acids Res.* **1990**, *18*, 6097–6100.
- (14) Pandey, A.; Mulder, D.; Ensign, S.; Peters, J. Structural basis for carbon dioxide binding by 2-ketopropyl coenzyme M oxidoreductase/carboxylase. *FEBS Lett.* **2011**, *585*, 459.
- (15) Kofoed, M. A.; Wampler, D. A.; Pandey, A. S.; Peters, J. W.; Ensign, S. A. Roles of the redox-active disulfide and histidine residues forming a catalytic dyad in reactions catalyzed by 2-ketopropyl coenzyme M oxidoreductase/carboxylase. *J. Bacteriol.* **2011**, *193*, 4904–4913.
- (16) Prussia, G. A.; Gauss, G. H.; Mus, F.; Conner, L.; DuBois, J. L.; Peters, J. W. Substitution of a conserved catalytic dyad into 2-KPCC causes loss of carboxylation activity. *FEBS Lett.* **2016**, *590*, 2991–2996.
- (17) Vögeli, B.; Geyer, K.; Gerlinger, P. D.; Benkstein, S.; Cortina, N. S.; Erb, T. J. Combining promiscuous acyl-CoA oxidase and enoyl-CoA carboxylase/reductases for atypical polyketide extender unit biosynthesis. *Cell Chem. Biol.* **2018**, *25*, 833–839.
- (18) Könnike, M.; Schubert, D. M.; Brown, P. C.; Hügler, M.; Standfest, S.; Schwander, T.; Schada von Borzyskowski, L.; Erb, T. J.

Stahl, D. A.; Berg, I. A. Ammonia-oxidizing archaea use the most energy-efficient aerobic pathway for CO<sub>2</sub> fixation. *Proc. Natl. Acad. Sci. U. S. A.* **2014**, *111*, 8239–8244.

(19) Berg, I. A.; Kockelkorn, D.; Buckel, W.; Fuchs, G. A 3-hydroxypropionate/4-hydroxybutyrate autotrophic carbon dioxide assimilation pathway in archaea. *Science* **2007**, *318*, 1782–1786.

(20) Tcherkez, G. G.; Farquhar, G. D.; Andrews, T. J. Despite slow catalysis and confused substrate specificity, all ribulose biphosphate carboxylases may be nearly perfectly optimized. *Proc. Natl. Acad. Sci. U. S. A.* **2006**, *103*, 7246–7251.

(21) Zhang, L.; Mori, T.; Zheng, Q.; Awakawa, T.; Yan, Y.; Liu, W.; Abe, I. Rational control of polyketide extender units by structure-based engineering of a crotonyl-CoA carboxylase/reductase in antimycin biosynthesis. *Angew. Chem.* **2015**, *127*, 13664–13667.

(22) Waterhouse, A.; Bertoni, M.; Bienert, S.; Studer, G.; Tauriello, G.; Gumienny, R.; Heer, F. T.; de Beer, T. A. P.; Rempfer, C.; Bordoli, L.; et al. SWISS-MODEL: homology modelling of protein structures and complexes. *Nucleic Acids Res.* **2018**, *46*, W296–W303.

(23) Flamholz, A.; Noor, E.; Bar-Even, A.; Milo, R. eQuilibrator—the biochemical thermodynamics calculator. *Nucleic Acids Res.* **2012**, *40*, D770–D775.

(24) Vögeli, B.; Erb, T. J. Negative' and 'positive catalysis': complementary principles that shape the catalytic landscape of enzymes. *Curr. Opin. Chem. Biol.* **2018**, *47*, 94–100.

(25) Rosenthal, R. G.; Vögeli, B.; Wagner, T.; Shima, S.; Erb, T. J. A conserved threonine prevents self-intoxication of enoyl-thioester reductases. *Nat. Chem. Biol.* **2017**, *13*, 745–749.

(26) Rétey, J. Enzymic reaction selectivity by negative catalysis or how do enzymes deal with highly reactive intermediates? *Angew. Chem., Int. Ed. Engl.* **1990**, *29*, 355–361.

(27) Erb, T. J.; Zarzycki, J. A short history of RubisCO: the rise and fall (?) of Nature's predominant CO<sub>2</sub> fixing enzyme. *Curr. Opin. Biotechnol.* **2018**, *49*, 100–107.

(28) Schada von Borzyskowski, L.; Rosenthal, R. G.; Erb, T. J. Evolutionary history and biotechnological future of carboxylases. *J. Biotechnol.* **2013**, *168*, 243–251.

(29) Zarzycki, J.; Brecht, V.; Muller, M.; Fuchs, G. Identifying the missing steps of the autotrophic 3-hydroxypropionate CO<sub>2</sub> fixation cycle in *Chloroflexus aurantiacus*. *Proc. Natl. Acad. Sci. U. S. A.* **2009**, *106*, 21317–21322.

(30) Zarzycki, J.; Fuchs, G. Coassimilation of organic substrates via the autotrophic 3-hydroxypropionate bi-cycle in *Chloroflexus aurantiacus*. *Appl. Environ. Microbiol.* **2011**, *77*, 6181–6188.

(31) Schwander, T.; Schada von Borzyskowski, L.; Burgener, S.; Cortina, N. S.; Erb, T. J. A synthetic pathway for the fixation of carbon dioxide *in vitro*. *Science* **2016**, *354*, 900–904.

(32) Trudeau, D. L.; Edlich-Muth, C.; Zarzycki, J.; Scheffen, M.; Goldsmith, M.; Khersonsky, O.; Avizemer, Z.; Fleishman, S. J.; Cotton, C. A.; Erb, T. J.; et al. Design and *in vitro* realization of carbon-conserving photorespiration. *Proc. Natl. Acad. Sci. U. S. A.* **2018**, *115*, E11455–E11464.